Three-dimensional photonic crystals containing designed defects achieved with two-photon photopolymerization

Ming Zhou (周 明)*, Wei Zhang (张 伟), Junjie Kong (孔俊杰), Haifeng Yang (杨海峰), and Lan Cai (蔡 兰)

Photonic Manufacturing Science and Technology Center and School of Materials Science and Engineering, Jiangsu University, Zhenjiang 212013

**E-mail: zm_laser@126.com*

Received June 2, 2008

Two-photon photopolymerization (TPP) with femtosecond laser is a promising method to fabricate three-dimensional (3D) photonic crystals (PCs). Based on the TPP principle, the micro-fabrication system has been built. The 3D woodpile PCs with rod space of 2000 nm are fabricated easily and different defects are introduced in order to form the cross-waveguide and the micro-laser structure PCs. Simulation results of the optical field intensity distributions using finite-difference time domain (FDTD) method are given, which support the designs and implementation of the PC of two types in theory.

OCIS codes: 320.7110, 060.4510, 250.2080, 250.5300.
doi: 10.3788/COL20090702.0165.

Photonic crystal (PC)[1], as a unique and promising photonic device, which is thought to be the most promising candidate to enable optical integration, has a periodic dielectric materials structure containing the photonic band gap (PBG) effect[2,3]. We have witnessed plenty of research efforts related to the fabrication techniques of PCs[4−7] in the past twenty years. Several groups have demonstrated that nonlinear optical lithography based on the two-photon photopolymerization (TPP) principle allows the fabrication of true three-dimensional (3D) nanostructures and 3D PCs[8−12].

In a process of TPP, an electron jumps from a ground state to an excited state by the simultaneous absorption of two laser photons[13]. With the focalization of laser beam in a transparent material, high light power is obtained in the focal spot region. Due to the Gaussian distribution of intensity at the focal spot and its quadratic dependence on the optical field intensity, by adjusting the laser power properly, one can make the exposure energy exceed a threshold, above which TPP can occur at the center of a Gaussian laser focal spot[14,15]. By moving the laser focus three dimensionally through the resin, any 3D structure with high resolution can be fabricated.

In our experiment, the output beam generated by an amplified Ti:sapphire laser system (homemade) with a pump source (Coherent) is attenuated by a half-wave plate/polarizer combination. After beam expansion, the laser pulses are coupled into an inverted biological microscope (Olympus). As shown in Fig. 1, the femtosecond laser pulses (30 fs, 82 MHz, 800 nm) are tightly focused into the volume of a photosensitive resin ORMOCER with a high numerical aperture (NA=1.35) oil immersion objective. The ORMOCER is placed on a 3D stage controlled by software for the positioning of the laser focus in the photosensitive resin. The charge-coupled device (CCD) camera mounted behind a dichroic mirror is employed for monitoring the TPP process online.

In order to increase the viscidity of the liquid resin, ORMOCER is baked for about 1 min in oven at 100 °C before the TPP process and about 3 min at the same temperature after the TPP. In the post processing, the 3D woodpile PCs can be gained after the unexposed resin is removed by washing in 4-methyl-2-pentanone about 1 min.

A sketch of the woodpile PC structure is shown in Fig. 2. It consists of layers of one-dimensional (1D) rods with a stacking sequence that repeats itself every four layers with a repetition distance of c. Within each layer, the axes of the rods are parallel to each other with an in-plane rod distance of a, and the lateral rod diameter is w. The orientations of the axes are rotated by 90° between the adjacent layers. Between the adjacent layers,

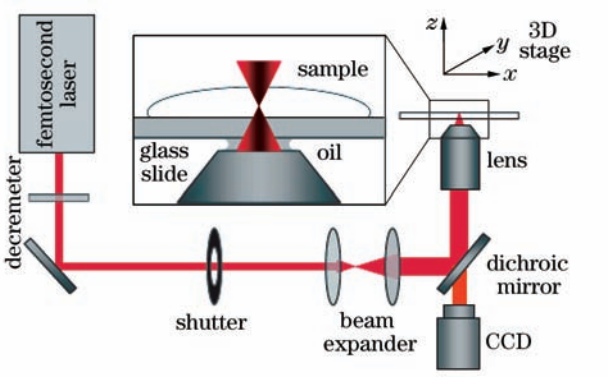

Fig. 1. 3D micro-fabrication system of TPP by femtosecond laser.

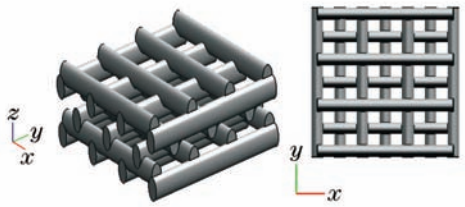

Fig. 2. Diagram of the 3D woodpile PC, the right figure is the planform image of the left one.

the rods are shifted relative to each other by $a/2$. For $(c/a)^2 = 2$, this 3D lattice exhibits a face-centered-cubic (f.c.c.) unit cell with a two-rod basis[16].

Figure 3 shows the scanning electron microscope (SEM) images of a typical PC fabricated by the microfabrication system in Fig. 1. The sample consists of 4 layers with an in-plane rod distance of $a = 2000$ nm and $(c/a)^2 \approx 2$. Many other PCs of larger areas have also been fabricated by TPP quickly. Figure 3 shows the panorama view with the area of 100×80 (μm), which is sufficiently large for optical spectroscopy measurement as well as for the use as potential devices. The enlarged view shows the woodpile stacking sequence and demonstrates the quality of our samples. In the enlarged view, a remaining roughness of 50 nm is visible and the lateral rod diameter is typically about 700 nm.

A linear defect and a dot in a PC can give rise to defect states within the bandgap and act as a waveguide and a micro-cavity, respectively. Light in the PC is confined to and guided along the channel or in the cavity because the PBG forbids light from escaping into the bulk crystal. We report different PC devices with the cross-waveguide (Fig. 4) and the micro-laser (Fig. 5) structures fabricated by TPP. All these samples have an in-plane rod distance of $a = 2000$ nm, 4 layers, and $(c/a)^2 = 2$ with an area of 20×20 (μm). In order to study the working principle of the cross-waveguide and the micro-laser PCs, we use the finite-difference time domain (FDTD) method to simulate the optical field intensity distributions of the two different structures. The model is set up based on the area of 20×20 (μm), the lateral rod diameter of 700 nm, the in-plane rod distance of $a = 2000$ nm with the elliptic rods. Firstly, we calculate the PBG of around 2.6 μm by FDTD. Secondly, a parallel beam with the wavelength of 2.6 μm is used to irradiate the models, which are designed as the cross-waveguide and the micro-laser structures mentioned above.

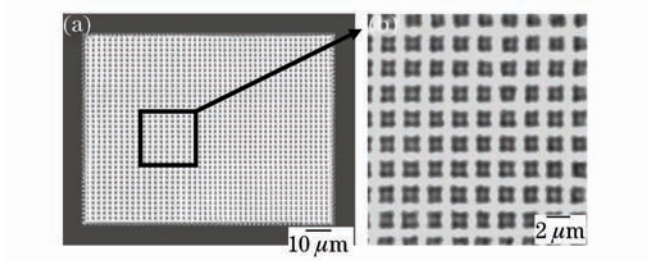

Fig. 3. 3D woodpile PC. (a) Panorama view; (b) partial enlarged view.

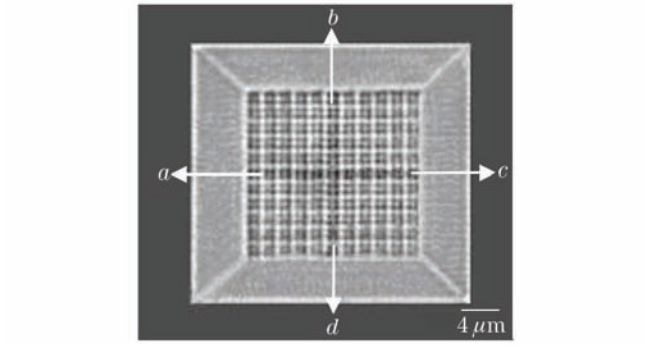

Fig. 4. Example of the cross-waveguide PC fabricated from ORMOCER.

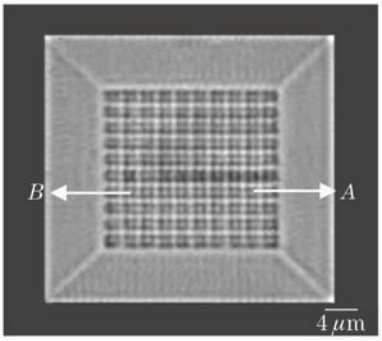

Fig. 5. Example of the new-style micro-laser PC fabricated from ORMOCER.

The laser parameters in TPP for the lateral rod diameter above are the laser power of 60 mW and the scanning speed of 80 μm/s. Meanwhile, we experimentally verify that with the fixed NA, the rod diameter decreases as the laser power decreases or the scanning speed increases. By contrary, the rod diameter increases as the others reverse, correspondingly. In order to achieve the high machining efficiency and the good PC qualities, we use the laser power ranging from 40 to 80 mW, and the scanning speeds from 60 to 120 μm/s to fabricate PCs. With the flexibility of the TPP method, we have fabricated a wide variety of lattice parameters with the in-plane rod distances ranging from 1000 to 3000 nm (not shown). All these indicate that TPP is an effective method to rapidly fabricate PCs with different in-plane rod distances.

In the cross sectional view of the cross-waveguide PC (Fig. 4), ac is the x direction waveguide and bd is the y direction waveguide (a, b, c, and d are marked in Fig. 4). The two cross waveguides intersecting each other are fabricated by removal of two rods of the adjacent layers in TPP. As Fig. 2 shows, the two waveguides are not in the same plane but separated from each other by $c/4$ in the z direction. Such asymmetry structure breaks the balance of the optical field distributions. A signal is imported in the port a and exported from c. Figure 6 shows the optical field distributions of the single-channel case, which validates the phenomena. The majority of the signal travels along the x direction and the minority transfers into the y direction. When signals in both directions are present, the signal in one direction may influence the signal transport in the other direction[17]. With PCs, it is possible to create waveguides that permit 90° bends with

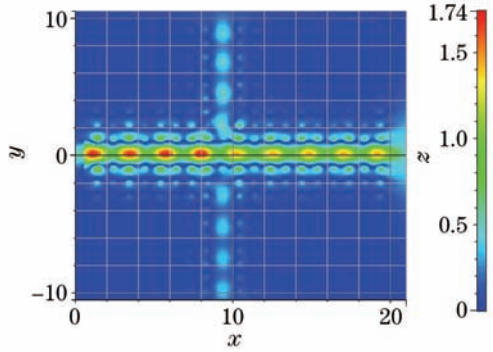

Fig. 6. Optical field intensity distributions of the cross-waveguide PC with single signal.

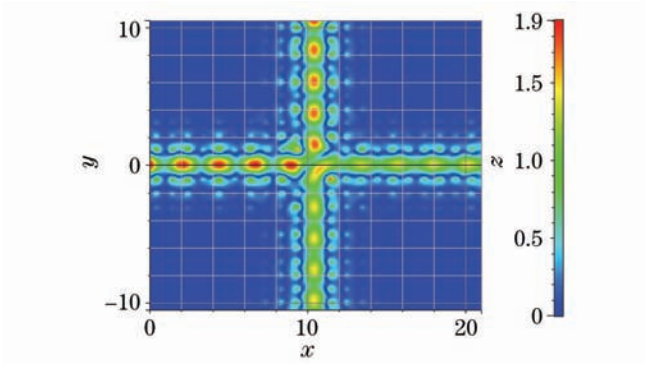

Fig. 7. Optical field intensity distributions of the cross-waveguide PC with double signals.

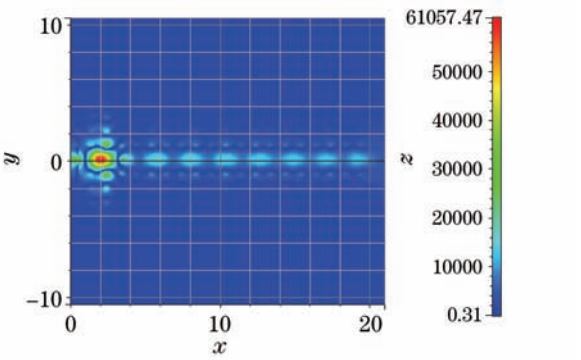

Fig. 8. Optical field intensity distributions of the new-style micro-laser PC.

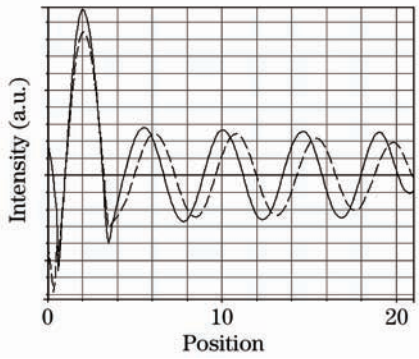

Fig. 9. Gaussian profile distributions of the new-style micro-laser PC. Solid line: actual curve; dashed line: ideal curve.

100% transmission. This phenomenon can be understood through the analogue of 1D resonant tunneling in quantum mechanics. The overlapping part of the two waveguides breaks the balance in the two directions and makes the two signals influence each other. Figure 7 shows the optical field intensity distributions of the two-channel case. The overlapping part may provide chances for the exchange of the signals. One signal in one direction may influence the signal in the other direction, which makes the two signals relative and controllable. It can be used as all-optical switch, optical isolator, optical transistor, and so on.

The quest for a compact micro-laser[18], with high quality factor and small mode volume, has been a central part of research in the field of integrated optics. The micro-lasers can be divided into three different types: point-defect laser, band-edge laser, and vertical cavity surface emitting laser (VCSEL)[19]. We develop a new 3D micro-laser structure. The section image of the fabricated new-style micro-laser PC (Fig. 5) with the waveguide structure in A and the micro-cavity structure in B (A and B are marked in Fig. 5). The waveguide and micro-cavity are fabricated in the same layer by removing parts of the rods in TPP. We can also control the width of cavities for different demands by changing the laser parameters of TPP. The high-quality optical micro-cavities with mode volumes far below a cubic wavelength have already been obtained, and can be used to obtain very high optical field intensities. In such a structure, the cavity may supply resonance for the light confined inside[20]. The emitted laser may propagate along the waveguide if some parameters are modified. Figure 8 shows the optical field distributions of the micro-laser PC, which verifies the above assumption. The most energy localization is in the cavity under resonance and amplification. There is some energy in the waveguide, which may be the laser overcoming the energy barrier and emitting out. Figure 9 is the optical field profile of the guided mode calculated in the cavity and the waveguide. The ideal curve and the actual one are both given in the figure. In the area of the cavity, the ideal and the actual curves accord with each other well, while in the area of the waveguide, some regular deviation appears due to the block between the two structures. We can adjust the structures of the cavity waveguide and block to avoid the deviation. Such new-style micro-laser PC may be useable as micro light sources in the future.

In conclusion, we report a promising method, TPP to fabricate 3D woodpile PCs and set up a 3D micro-fabrication system. With direct femtosecond laser writing[21], TPP has been realized in a photosensitive resin ORMOCER, and different 3D woodpile PCs with the in-plane rod distance $a = 2000$ nm have been fabricated. Simulation results of the optical field distributions are given by using the method based on FDTD.

This work was supported by the National Natural Science Foundation of China (No. 50375068 and 50775104), the Foundation for the Author of National Excellent Doctoral Dissertation of China (No. 96039), and the Natural Science Foundation of Jiangsu Province.

References

1. E. Yablonovitch, Phys. Rev. Lett. **58,** 2059 (1987).
2. Z. Tian, C. Wang, Y. Li, Q. Xing, Y. Song, M. Hu, L. Chai, and Q. Wang, Chinese J. Lasers (in Chinese) **35,** 477 (2008).
3. J. Yin, X. Huang, and S. Liu, Chinese J. Lasers (in Chinese) **34,** 1077 (2007).
4. E. Yablonovitch, T. J. Gmitter, and K. M. Leung, Phys. Rev. Lett. **67,** 2295 (1991).
5. M. Qi, E. Lidorikis, P. T. Rakich, S. G. Johnson, J. D. Joannopoulos, E. P. Ippen, and H. I. Smith, Nature **429,** 538 (2004).
6. A. Blanco, E. Chomski, S. Grabtchak, M. Ibisate, S. John, S. W. Leonard, C. Lopez, F. Meseguer, H. Miguez, J. P. Mondia, G. A. Ozin, O. Toader, and H. M. van Driel, Nature **405,** 437 (2000).
7. M. Campbell, D. N. Sharp, M. T. Harrison, R. G. Denning, and A. J. Turberfield, Nature **404,** 53 (2000).

8. S. Kawata, H.-B. Sun, T. Tanaka, and K. Takada, Nature **412,** 697 (2001).
9. H.-B. Sun, S. Matsuo, and H. Misawa, Appl. Phys. Lett. **74,** 786 (1999).
10. M. Deubel, G. von Freymann, M. Wegener, S. Pereira, K. Busch, and C. M. Soukoulis, Nature Mater. **3,** 444 (2004).
11. J. Serbin, A. Ovsianikov, and B. Chichkov, Opt. Express **12,** 5221 (2004).
12. M. Straub and M. Gu, Opt. Lett. **27,** 1824 (2002).
13. Y. R. Shen, *Principles of Nonlinear Optics* (Wiley, New York, 1984).
14. S. Kawata and H.-B. Sun, Appl. Surf. Sci. **208,** 153 (2003).
15. J. Qiu, K. Miura, and K. Hirao, Proc. SPIE **5350,** 1 (2004).
16. S. Y. Lin, J. G. Fleming, D. L. Hetherington, B. K. Smith, R. Biswas, K. M. Ho, M. M. Sigalas, W. Zubrzycki, S. R. Kurtz, and J. Bur, Nature **394,** 251 (1998).
17. M. Soljačić and J. D. Joannopoulos, Nature Mater. **3,** 211 (2004).
18. H.-G. Park, S.-H. Kim, S.-H. Kwon, Y.-G. Ju, J.-K. Yang, J.-H. Baek, S.-B. Kim, and Y.-H. Lee, Science **305,** 1444 (2004).
19. K. Inoue and K. Ohtaka, (eds.) *Photonic Crystals: Physics, Fabrication and Applications* (Springer, Berlin, 2004).
20. S. Ogawa, M. Imada, S. Yoshimoto, M. Okano, and S. Noda, Science **305,** 227 (2004).
21. F. He and Y. Cheng, Chinese J. Lasers (in Chinese) **34,** 595 (2007).